a total body electrocardiographic surface map: Adult male torso simulation with lungs. Circulation **38:** 684-690, 1968
3. d'Alche P, Ducimetiere P, Lacombe J: Computer model of cardiac potential distribution in an infinite medium and on the human torso during ventricular activation. Circ Res **34:** 719-729, 1974
4. Harumi K, Burgess MJ, Abildskov JA: A theoretic model of the T-wave. Circulation **34:** 657-688, 1966
5. Thiry PS, Rosenberg RM: On electrophysiological activity of the normal heart. J Franklin Inst **297:** 377-396, 1974
6. Spach MS, Barr RC, Serwer GA, Kootsey JM, Johnson EA: Extracellular potentials related to intracellular action potentials in the dog Purkinje system. Circ Res **30:** 509-519, 1972
7. Spach MS, Barr RC: Origin of epicardial ST-T wave potentials in the intact dog. Circ Res **39:** 475-487, 1976
8. Durrer D, van Dam RT, Freud GE, Janse MJ, Meijler FL, Arzbaecher RC: Total excitation of the isolated human heart. Circulation **41:** 899-912, 1972
9. Solomon MS, Selvester MD: Simulation of measured activation sequence in the human heart. Am Heart J **85:** 518-523, 1973
10. Burgess MJ, Green LS, Millar K, Wyatt R, Abildskov JA: The sequence of normal ventricular recovery. Am Heart J **84:** 660-669, 1972
11. Arthur RM: Evaluation and use of a human dipole plus quadrupole equivalent cardiac generator. Ph.D. Dissertation, University of Pennsylvania, 1968
12. Swihart JC: Numerical methods for solving the forward problem in electrocardiography. *In* The Theoretical Basis of Electrocardiology, edited by CV Nelson, DB Geselowitz. London, Oxford University Press, 1976, pp 257-293
13. Cuffin BN, Geselowitz DB: Studies of the electrocardiogram using realistic cardiac and torso models. IEEE Trans Biomed Eng **24:** 242-252, 1977
14. Taccardi B: Distribution of heart potentials on the thoracic surface of normal human subjects. Circ Res **12:** 341-352, 1963
15. Taccardi B: Body surface distribution of equipotential lines during atrial depolarization and ventricular repolarization. Circ Res **19:** 865-878, 1966
16. Lynn MS, Barnard ACL, Holt JH, Sheffield LTA: A proposed method for the inverse problem in electrocardiology. Biophys J **7:** 925-945, 1967
17. Samson WE, Scher AM: Mechanism of ST segment alteration during acute myocardial injury. Circ Res **8:** 780-787, 1960
18. Crill WE in Woodbury JW: Cellular electrophysiology of the heart. *In* Handbook of Physiology, section 2, Circulation, vol 1, edited by WF Hamilton, P Dow. Washington, D.C., American Physiological Society, 1962, p 237
19. Sperelakis N, MacDonald RL: Ratio of transverse to longitudinal resistivities of isolated cardiac muscle fiber bundles. J Electrocardiol **7:** 301-314, 1974

Simulation Studies of the Electrocardiogram

II. Ischemia and Infarction

WALTER T. MILLER, III, AND DAVID B. GESELOWITZ

SUMMARY **Experimental studies of the myocardial action potential following coronary artery occlusion have shown that the resulting regional ischemia is reflected by characteristic changes in the shapes of the action potentials in the ischemic region. The principal changes are decreases in the magnitude of the resting potential and in the action potential duration. Action potentials with prolonged durations have been observed in the infarcted regions of experimental animals after the development of inverted T waves in the surface electrocardiogram (ECG). We use such abnormal action potentials in our digital computer model to study the effects of acute myocardial ischemia and infarction on the surface ECG. The heart is represented in sufficient detail to allow variations in the location and size of the ischemic injury and in the distribution of the severity of injury within the injured region. The evolution of acute infarctions is simulated by progressively modifying the abnormal action potentials assigned to the injured region. Calculated standard 12 lead ECGs and torso isopotential surface maps for simulated acute ischemia and infarction are in good agreement with patient data reported in the literature. Typical simulations include anterior and inferior transmural ischemia and infarction and anterior subendocardial ischemia. The model is used to examine relationships between torso surface potentials during ventricular activation and recovery and the site and size of the ischemic injury.**

THE electrocardiogram (ECG) has long been recognized as an important aid in the diagnosis and localization of myocardial ischemia and infarction. Characteristic changes in the QRS complexes, S-T segments, and T waves recorded from standard leads have been described for various stages of acute and chronic myocardial infarction.[1] S-T segment and T wave changes during exercise testing are significant indicators of ischemia resulting from coronary insufficiency. In addition to these qualitative tests, body surface mapping techniques are currently being studied in an effort to provide more accurate information concerning the location and extent of myocardial injury.[2]

In spite of their widespread clinical and experimental use in the study of ischemia and infarction, the relationships between the changes in the surface ECG and the evolution of the injury at the cellular level are not clearly understood. Experimental studies have shown that characteristic changes take place in the shapes of cellular transmembrane action potentials recorded near the center of the injured region following an acute occlusion of

From the Bioengineering Program, The Pennsylvania State University, University Park, Pennsylvania.

Supported by a grant from the American Heart Association, Pennsylvania Affiliate and Mideastern Pennsylvania Chapter.

Address for reprints: Dr. David B. Geselowitz, Bioengineering Program, Pennsylvania State University, University Park, Pennsylvania 16802.

Received July 18, 1977; accepted for publication March 22, 1978.

a coronary artery.[3,4] In general, there are progressive decreases in the magnitudes of the resting potentials, in the action potential durations, and in the rates of depolarization, until no action potentials can be elicited. The exact mechanisms responsible for these action potential changes are not known, although hypoxia, acidosis, and increased extracellular potassium appear to be contributing factors.[5] If the injured area is reperfused within minutes after the initial occlusion, the "injured" action potentials return to normal, the decreased action potential durations generally persisting longer after the reperfusion than the decreased resting potentials. If the occlusion is maintained for a period of hours, permanent cell damage occurs, leading to eventual cell death.

Few data are available concerning the action potential changes which occur in surviving cells in the injured region hours, days, or weeks after a coronary occlusion. Myocardial cells with prolonged action potential durations have been observed in infarcted regions following the development of inverted T waves in the surface ECG.[6] The relationships between these prolonged action potentials and the shortened action potentials observed immediately following a coronary occlusion are not known.

Each of the action potential changes cited can be associated with particular types of changes in the surface ECG. For example, decreased resting potentials in the injured region result in baseline shifts in the potential waveforms recorded at the surface. Since electrocardiographic amplifiers are commonly AC coupled, the baseline is seen as the potential reference and the baseline shifts appear as reciprocal changes in the S-T segment, termed "secondary" S-T segment shift. Shortened action potential durations result in true or "primary" S-T segment shifts and T wave changes in the same direction as the S-T segment shifts.[7] Such qualitative relationships can be used to predict the types of changes in the surface ECG that can be expected for given types of abnormal action potentials in the injured region. Myocardial injuries generally have complex and irregular geometries, however, and vary greatly in location, size, and in the distribution of the severity of injury within the injured region. It is impossible to predict accurately the nature of the changes in the surface ECG without taking all of these factors into account. In addition, volume conductor distance and boundary effects in the torso must be considered.

In the preceding paper, we reported a digital computer model for the simulation of torso surface potentials during both ventricular activation and recovery starting from assumed distributions of cellular action potentials within the myocardium. Various stages of ischemia and infarction can be simulated with this model by appropriately modifying the action potentials assigned to the injured region. The ventricles of the heart are represented in sufficient detail to allow variations in the location and size of the myocardial injury. Torso surface potentials resulting from complex combinations of tissue necrosis and abnormal action potentials within the injured region can be simulated. The purpose of our study was to examine whether "realistic" myocardial injuries based on abnormal action potentials reported in the literature could be used in the model to account for the types of abnormal electrocardiograms observed during different stages of ischemia and infarction.

Methods

Detailed descriptions of the model and the techniques used for calculating surface potentials are presented in the preceding paper on normal heart simulation. Ischemia and infarction were simulated by altering the shapes of the transmembrane action potentials assigned to the injured regions of the heart model. The transmembrane action potential at each point in the model was defined by four parameters: the resting potential, the maximum depolarization potential, the action potential duration, and the depolarization rise time. Abnormal action potentials were implemented by specifying changes in these four parameters from their normal values. The breakpoints used to define the line segments in the action potential model were then adjusted in proportion to the changes in these time and voltage parameters.

Increasing severity of ischemia was simulated by progressively decreasing the magnitude of the resting potential, the action potential duration, and the maximum depolarization potential, while increasing the depolarization rise time. In the most severe stage of ischemia, it was assumed that no action potential was elicited and the transmembrane potential was held at the constant value of −60 mV. Figure 1 shows four typical action potentials in various stages of ischemia. Prolonged action potentials in infarcted regions were simulated by increasing the action potential duration, while leaving the other parameters the same as in the normal heart simulation. Necrotic tissue in infarction was taken to be electrically inactive and was simulated by removing the corresponding points from the heart model.

The distribution of the severity of the injury within a particular injured region was modeled by dividing the injury into five segments running from the periphery (segment 1) to the central portion of the injury (segment 5) as shown in Figure 2A. Normal regions were assigned a segment number 0. In a given simulation, each of the

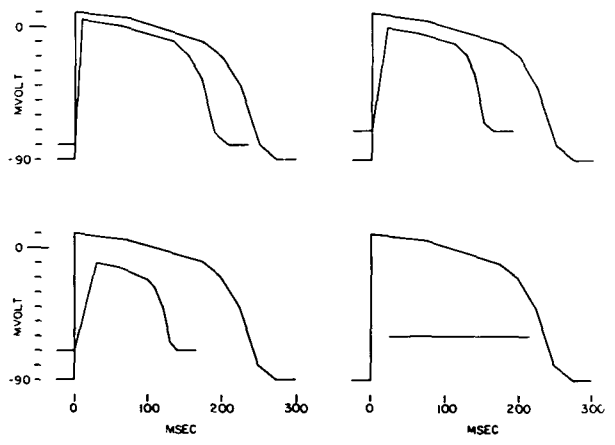

FIGURE 1 *"Ischemic" action potentials as used in the simulations. A normal action potential is shown in each segment as a reference.*

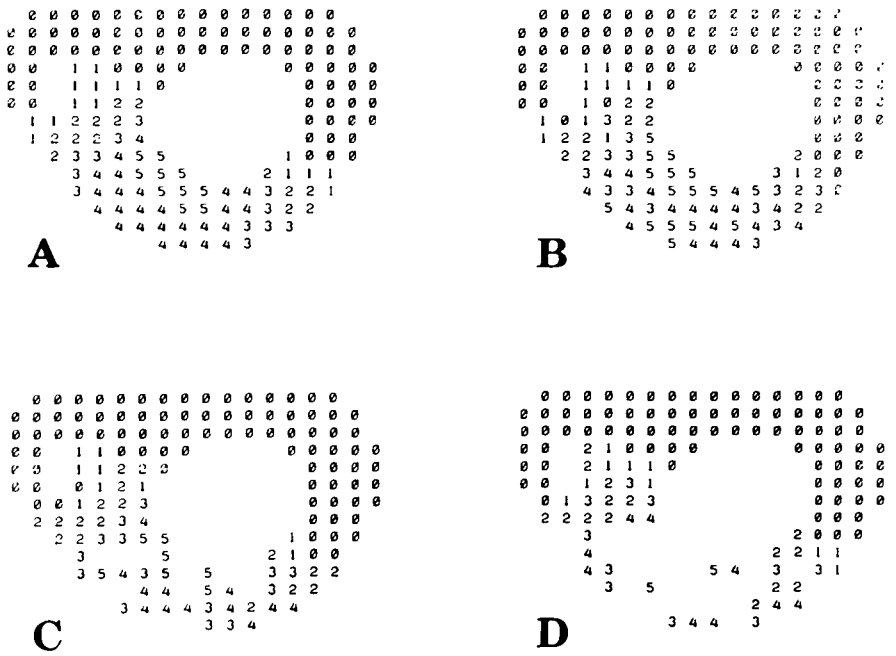

FIGURE 2 *A cross-section of a simulated injury in the anterior wall of the left ventricle. A: The injury as originally assigned showing the five segments running from the periphery to the central portion of the injured region. B: The same injury in a particular simulation after randomization (see text). The numbers 1-5 represent action potentials with increasing severity of injury. C: The injury in a simulation including "patchy" necrosis. Missing array points indicate simulated necrotic regions. D: The injury in a simulation involving extensive necrosis.*

five segments of an injury was assigned a percentage of tissue necrosis and a set of changes in the four action potential parameters. The computer then used these data to assign an action potential to each point in the injured region of the heart model. For example, if segment 3 were specified as having 20% tissue necrosis, the computer would first randomly eliminate 20% of the points in segment 3. All of the surviving points in segment 3 would then be assigned the same set of *changes* in the four action potential parameters. The action potential at each point in segment 3 would then be determined by the four normal parameters for that particular point, modified by the action potential changes characterizing segment 3.

The division of each injury into five segments allowed the simulation of injuries that were graded in severity from the periphery to the central portion. Initial simulations were performed using five discrete segments as shown in Figure 2A. The resulting surface electrocardiograms occasionally showed abrupt changes that were judged to be artifacts of the distinct boundaries separating different regions of the injury. To eliminate the effects of these distinct boundaries, the injuries were randomized in the following manner. The segment numbers of 20% of the points in each injury were increased by one, the segment numbers of 20% of the points in each injury were decreased by one, and the segment numbers of the remaining 60% of the points were left at their original values. Points with a resulting segment number of 6 were assigned to segment 5.

This randomization of each injury eliminated the distinct boundaries separating different segments of the injury, but preserved the general increase in segment number from the periphery to the central portion of the injury (Figure 2, B-D). Potential waveforms calculated using the randomized injuries had essentially the same shape as those obtained using the five distinct segments, but were generally smoother in form. Randomizations of the same injury using different sets of random numbers resulted in only minor differences in the shapes of the potential waveforms. The principal effect of the randomization procedure was thus to smooth the calculated surface potential waveforms.

Slowed conduction in the injured region during severe ischemia was simulated by adding an activation delay to the activation times of points in the injured region. The activation delay was assumed to vary approximately as the square of the distance from the edge of the injury to the central portion, and linearly with distance from the endocardium to the epicardium. The greatest delay was thus at the center of the injury near the epicardium. Activation times in the normal portions of the myocardium were assumed to be unaffected by the injuries. No overall changes in activation sequence caused by ischemia and infarction were simulated.

Results

Figure 3 shows 15 cross-sections of the heart model with a simulated injury in the anterior wall of the left ventricle. The injury is shown divided into three segments to emphasize that the severity of the injury was graded from the periphery to the central portion of the injured region. The exact nature of the gradation, however, was more complex than is implied by the three segments (Fig. 2). Calculated standard 12-lead electrocardiograms sim-

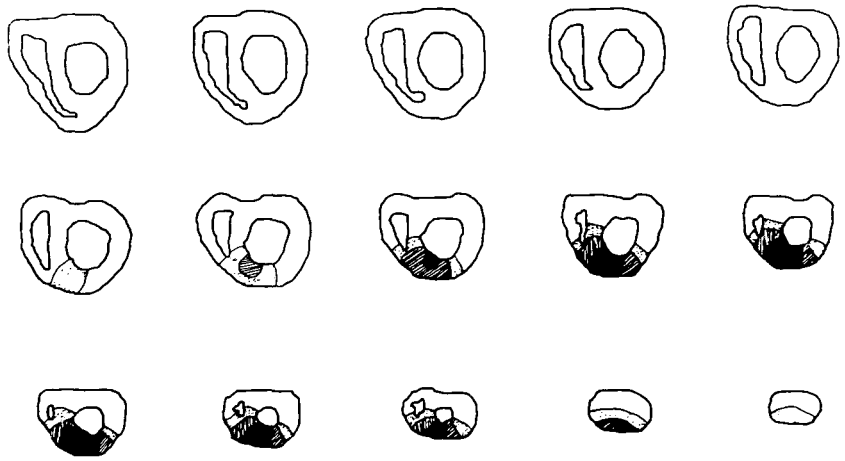

FIGURE 3 *A simulated injury in the anterior wall of the left ventricle. The heart model is shown in 15 cross-sections shifting from base to apex, as viewed from left to right and top to bottom. The three divisions of the injury indicate the approximate boundaries. The detailed distributions of the severity of injury were more complex (Fig. 5).*

ulating four stages in the evolution of a myocardial infarction in this anterior location are presented in Figure 4.

The first simulation (Fig. 4A) represents the early ischemic phase of the infarction with action potentials in the injured region similar to the two less severely injured forms shown in Figure 1. The dash at the beginning of each waveform indicates the true zero potential level. It can be seen that most of the early S-T segment elevation in the precordial leads was a reflection of the depression of the baseline caused by the altered transmembrane resting potentials. Tall T waves were present in the precordial leads as a result of the shortened action potential durations. Delayed activation in the injured region (with a maximum delay of 20 msec) resulted in changes in the QRS complexes, including delays in the peaks of the R waves in V2-V6 with subsequent decreases in magnitude or disappearance of the S waves.

The ECG shown in Figure 4B corresponds to a simulation in which it was assumed that the central portion of the injury contained action potentials similar in shape to the more severely injured forms shown in Figure 1, mixed with a small percentage of tissue necrosis. Locations near the edge of the injury tended to have action potentials with durations 40–80 msec longer than normal. Extreme S-T segment elevation and inverted T waves are evident in leads I, aVL, and V2-V6. The combination of activation delay (with a maximum delay of 30 msec) and action potentials with decreased magnitudes resulted in further changes in the QRS complexes with the development of Q waves in aVL and V3-V6.

The next step in the simulated evolution of an anterior infarction involved an injury composed of extensive tissue necrosis mixed with cells having prolonged action potential durations. The abnormal features in the calculated 12-lead ECG (Fig. 4C) included prominent Q waves in leads I, aVL, and V2-V6, with notching in V4. Wide, deeply inverted T waves were evident in the same leads. The S-T segments were nearly isoelectric in all leads.

In the final stage of the simulated infarction (Fig. 4D)

FIGURE 4 *Standard 12-lead electrocardiograms resulting from the simulated evolution of an anterior transmural infarction. The horizontal and vertical calibration lines indicate 0.4 second and 1.0 mV, respectively.*

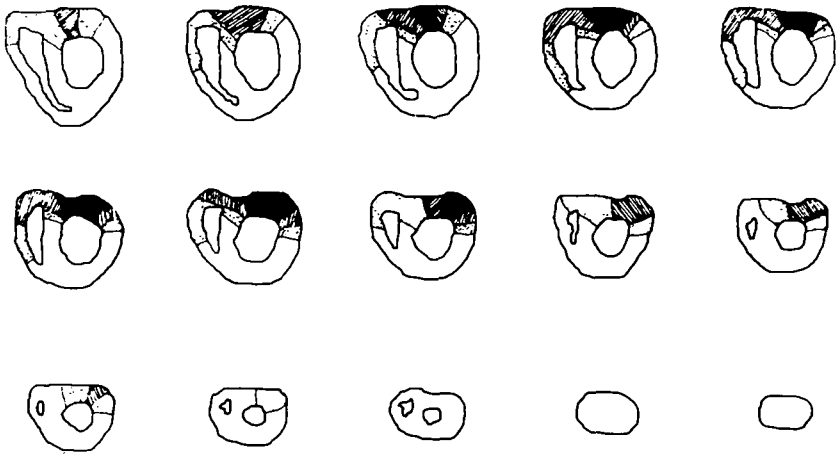

FIGURE 5 *A simulated injury in the inferior wall of the left ventricle.*

it was assumed that the action potential shapes of the surviving cells in the injured region had returned to normal. The same tissue necrosis was present as in the injury associated with Figure 4C. It can be seen that while the Q waves resulting from the necrosis persisted from the previous stage of the simulated injury, the previously inverted T waves returned to their normal polarity, although they were generally smaller in magnitude than in the normal heart simulation. This clearly associates the inverted T waves in the simulation with the prolonged action potentials assigned to the injured region. An infarction in the inferior left ventricle is presented in Figure 5 and the ECGs in Figure 6 show four stages in the simulated evolution of the infarct. The transmembrane action potentials assigned to the injured region were similar to those used in the respective stages of the anterior infarction, with the following exceptions. In the second stage of the infarction (Fig. 6B), no action potentials with prolonged durations were used, and as a result T wave inversions did not occur in the leads showing S-T segment elevations. In the third stage (Fig. 6C), a small number of sites with "ischemic" action potentials (Fig. 1) existed toward the center of the injured region, resulting in low magnitude S-T segment deviations. Similar changes in the QRS complexes, S-T segments, and T waves can be seen in the corresponding stages of the simulated anterior and inferior infarctions when differences in locations between the two regions are taken into account.

Subendocardial ischemia was simulated in an anterior location similar to that shown in Figure 3. Figure 7A shows the 12-lead ECG resulting from a simulation in which action potentials with decreased resting potentials (from 0 to 20 mV less than normal) were assigned to the subendocardial injury. Horizontal S-T depression is seen in leads I, aVL, and V2-V5, reflecting baseline elevation in the same leads. In the simulation shown in Figure 7B, it was assumed that the action potentials in the injured region had shortened durations (from 0 to 40 msec less than normal) with normal resting potentials. Decreased

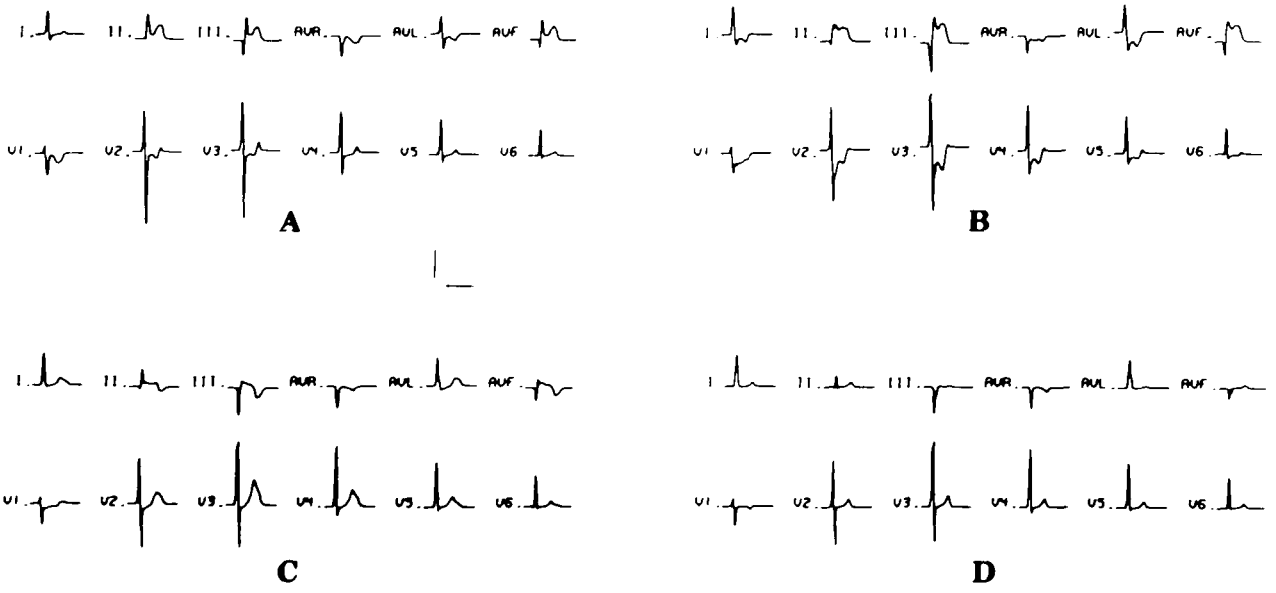

FIGURE 6 *Standard 12-lead ECGs resulting from the simulated evolution of an inferior transmural infarction. The horizontal and vertical calibration lines indicate 0.4 second and 1.0 mV, respectively.*

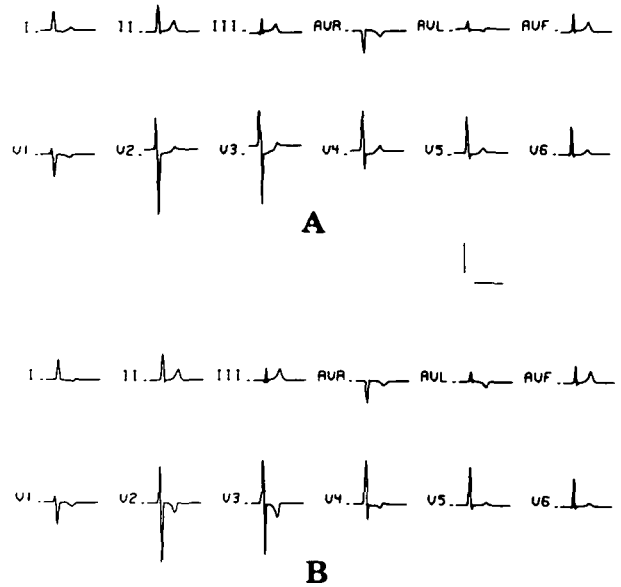

FIGURE 7 *Standard 12-lead ECGs resulting from simulated anterior subendocardial ischemia. The horizontal and vertical calibration lines indicate 0.4 second and 1.0 mV, respectively.*

or inverted T waves are apparent in the leads with have S-T segment depression in Figure 7A. The shortened action potential durations in the subendocardial injury altered the normal transmural gradient of durations, resulting in inverted T waves.

In Figure 8, two anterior injuries are shown with the

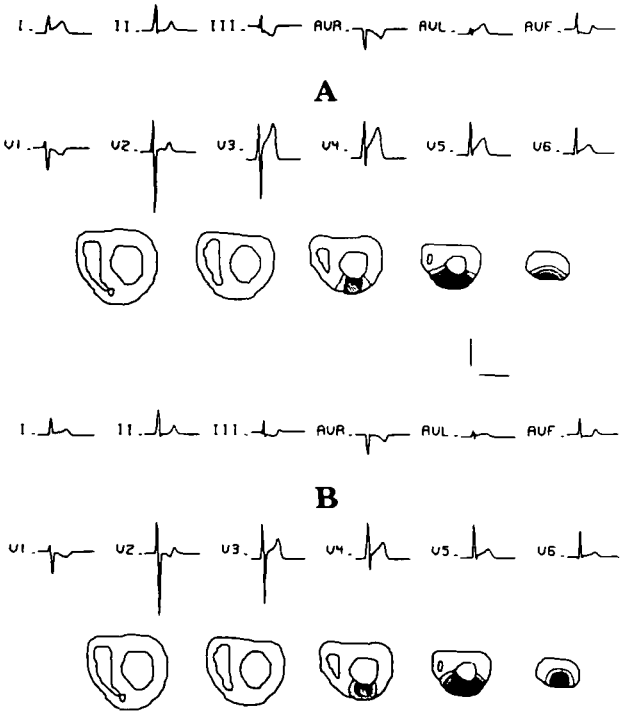

FIGURE 8 *Standard 12-lead ECGs resulting from simulated anterior transmural ischemias. The approximate boundaries of the injuries are shown on the five cross-sections of the heart model below each ECG. The horizontal and vertical calibration lines indicate 0.4 second and 1.0 mV, respectively.*

calculated 12-lead ECGs resulting from simulated ischemia in the injured areas. The two injuries were designed so that they were located in the same portion of the wall of the left ventricle and occupied approximately the same volume of the myocardium. The types of "ischemic" action potentials assigned to the two injured regions were identical. The only differences between the two regions were in the shapes of the boundaries defining the injuries. A comparison of the two electrocardiograms shows that the minor differences in geometry were sufficient to cause a factor of two differences in the magnitudes of the calculated S-T segment and T wave changes.

It is important to note that the model is not limited to the simulation of standard 12-lead ECGs. Potentials can be calculated anywhere on the torso surface. Figure 9 shows three torso isopotential surface maps calculated 30 msec after the beginning of the activation sequence for the normal heart simulation, a simulated anterior infarction, and a simulated inferior infarction. Both simulated infarctions included extensive tissue necrosis in the injured regions. In Figure 9B, the potential maximum is displaced from its normal position and an abnormal minimum is present on the torso, near the infarcted region in the anterior left ventricle. The simulated inferior infarction (Fig. 9C) did not result in such a distinct abnormal feature, but the potential minimum was displaced from its normal position near the right shoulder to the lower right region of the torso.

The isopotential surface maps in Figure 10 represent the calculated distributions of torso surface potentials early in the S-T segment corresponding to simulated transmural ischemias in the anterior, lateral, and inferior walls of the left ventricle, and to a simulated anterior subendocardial ischemia. In each of the maps resulting from a transmural ischemia there is a potential maximum on the portion of the torso facing the injury, and an opposing potential minimum. The exact placement of these maxima and minima is dependent on both the locations of the injuries and the distance effects in the torso. Thus, the opposing maxima and minima are not necessarily on opposite sides of the torso. The potential distribution resulting from the anterior subendocardial ischemia is very similar to that resulting from the anterior transmural ischemia, with the positions of the maximum and minimum reversed.

Discussion

Few theoretical studies have been reported concerning the relationships between the changes in the surface ECG during ischemia and infarction and the underlying changes in the electrical activity of the myocardial cells in the injured region. In a simulation study, Thiry[8] demonstrated that cellular transmembrane action potentials of reduced amplitude could be used to explain the polarity of the S-T segment deviations in standard 12-lead electrocardiograms resulting from anterior and inferior ischemia. The study was based on a simplified heart model located in an infinite homogeneous conductive medium, however, and was limited in scope. In our model, the ventricles of a human heart are represented in detail and

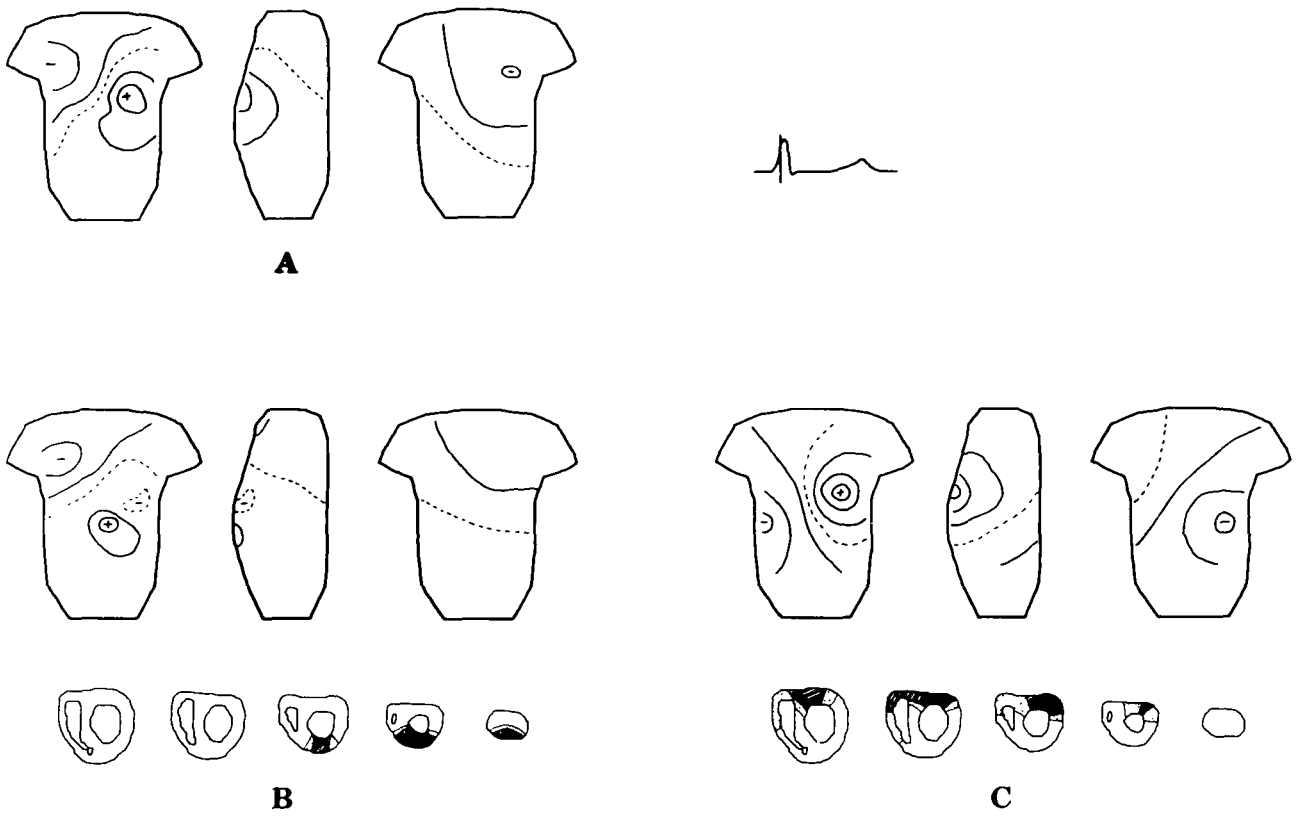

FIGURE 9 *Simulated isopotential surface maps 30 msec after the beginning of ventricular activation. The torso is shown in front, left side, and rear views. The positions of relative maxima and minima are indicated by the "+" and "−" characters, respectively. The lines of zero potential are shown as broken lines. A: The surface map resulting from the normal heart simulation. A lead II ECG is shown to provide a time reference. B: The surface map resulting from a simulated anterior infarction. The approximate location of the injury is shown on the five cross-sections of the heart model. C: The surface map resulting from a simulated inferior infarction.*

are taken to be located in a torso with realistic surface boundaries. Complex distributions of action potential shapes can be simulated and the resulting electrocardiograms calculated at any point on the torso surface. The results presented indicate that "realistic" injuries based on information from experimental studies reported in the literature can be used in the model to simulate surface electrocardiograms for various stages and locations of ischemia and infarction. The model should thus be useful in the study of the electrocardiographic abnormalities resulting from such myocardial injuries.

The earliest electrocardiographic signs of acute transmural myocardial infarction (as seen by leads facing the injury) include S-T segment elevation, peaking of the T wave, a delay in the peak of the R wave with a possible increase in magnitude, and a decrease in magnitude or disappearance of the S wave.[9] In some cases "giant" R waves have been observed. With the exception of the giant R waves, all of these features are present in the precordial leads of the 12-lead ECG calculated for the first stage of the simulated anterior infarction (Fig. 4A). In the simulation the S-T segment, elevations at this stage of the injury were primarily the reflections of baseline depressions caused by the altered resting potentials, and the peaked T waves arose from the shortened action potential durations. The QRS complex changes resulted from delayed activation in the injured region. Because of the large degrees of source cancellation during ventricular activation, relatively small delays in the activation of a particular region of the myocardium can have dramatic effects on the ECG. The delayed activation in the anterior injury resulted in a merging of the R and S waves in the precordial leads (Fig. 4A) and a subsequent disappearance of the S waves in leads V3-V6. A similar activation delay in the inferior injury resulted in a separation of the R and S waves in the precordial leads (Fig. 6A) with corresponding increases in magnitude. The same mechanism can be proposed as the source of the giant R waves. If the activation delay in an injured region is such that the positive source components persist while the negative components in the opposite wall are decaying, large R waves could result.

Inversions of the T waves in leads previously showing S-T segment elevations are characteristic signs of myocardial infarction.[1] These inverted T waves are often deep and wide. Although the mechanisms responsible for such T wave changes have not been positively identified, cells with prolonged action potential durations have been observed in the infarcted regions of experimental animals following the development of inverted T waves in the surface ECG.[6] Action potentials with durations 40–80 msec longer than normal were used in the simulations

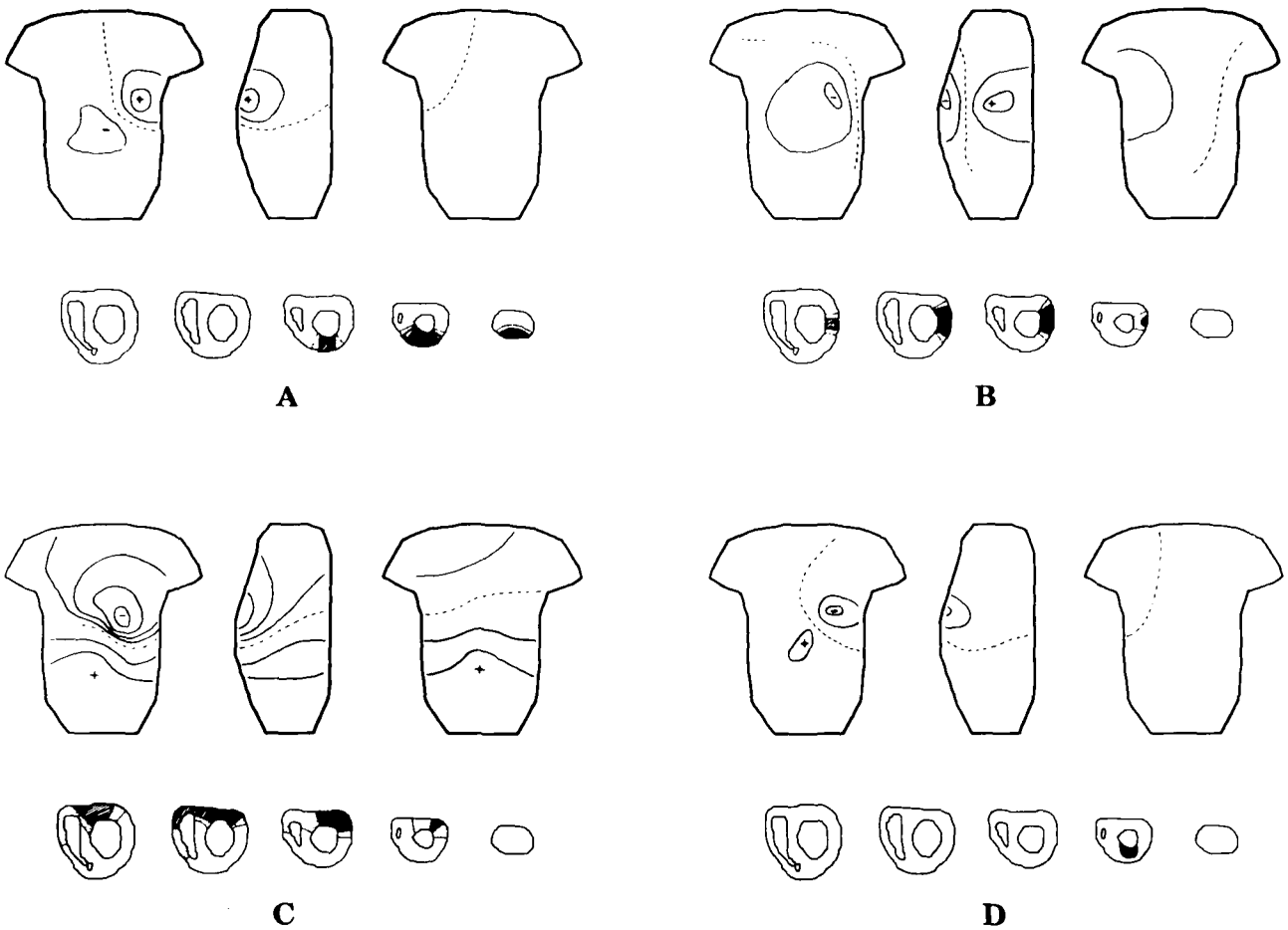

FIGURE 10 *Calculated isopotential surface maps at the beginning of the S-T segment for four simulated ischemias. The approximate location of each injury is shown on the five cross-sections of the heart model below the respective map.*

(Fig. 4, B and C, and Fig. 6C) to produce T wave inversion. Note that extensive tissue necrosis alone, without cells with prolonged action potential durations, was not sufficient to produce major T wave changes (Figs. 4D and 6D).

The appearance of prominent Q waves in the ECG following myocardial infarction is commonly associated clinically with the development of tissue necrosis in the injured region.[1] This association is supported by the simulation results. In both the simulated anterior and inferior infarctions, Q waves developed in the appropriate leads when significant tissue necrosis in the injured region was assumed. Notice, however, the Q waves in leads III and aVF in the first stage of the simulated inferior infarction (Fig. 6A). These Q waves arose as a direct result of the simulated delayed activation in the injured region, indicating that the first appearance of Q waves in the surface ECG following myocardial infarction may not necessarily signal the development of inactive or necrotic tissue in the injury. It is interesting to note that in an early paper describing the abnormal Q wave in chronic myocardial infarction, Fenichel[10] attributed the Q waves to delayed activation rather than loss of active tissue in the infarcted region.

S-T segment depression during and immediately following exercise testing has been shown to be a significant indicator of myocardial ischemia resulting from coronary insufficiency.[1] Often S-T segment depression will develop during the exercise period, followed, upon relaxation, by a decrease in depression with T wave inversion in the same leads and, finally, a return of the ECG to normal. Experimental studies have indicated that the first changes in cellular action potentials during ischemia are decreases in the transmembrane resting potentials, followed by decreases in action potential durations.[3] There is also evidence that, upon reperfusion, the decreased resting potentials may return toward normal before the decreased action potential durations.[4] In the simulated anterior subendocardial ischemia (Fig. 7), S-T segment depression developed as the result of decreased resting potentials in the injured region, and T wave inversion developed as the result of shortened action potential durations. This suggests a mechanism for the appearance first of S-T segment depression and then T wave inversion following exercise testing. As ischemia develops as a result of the exercise, the resting potentials of cells in the ischemic region begin to decrease, resulting in horizontal S-T segment depressions in leads over the injured region. The action potential durations of the same cells then start to decrease with corresponding T wave inversions.

The S-T segment depressions merging into the inverted T waves result in patterns known as "down-sloping" S-T segment depression. Upon reperfusion of the ischemic region, the decreased resting potentials, and the corresponding S-T segment depressions, return toward normal, leaving distinct inverted T waves. The action potential durations then return toward normal and the T waves return to their original polarity.

In a combined theoretical and experimental study, Holland[11] demonstrated that S-T segment deviations were dependent on the locations of the measuring electrodes with respect to the boundaries separating the normal and ischemic regions of the myocardium, rather than on the volume of the ischemic region. In a realistic injury there are spatial variations in the severity of ischemia, and the boundaries of interest are distributed throughout the injured region. Similar relationships exist between these distributed boundaries and the observed S-T segment deviations, as is evident in the simulations shown in Figure 8. Both simulated injuries were in approximately the same location, had nearly the same volume, and were assigned the same abnormal action potentials. The shapes of the boundaries defining the two injuries were different, however, and as a result the S-T segment shifts from one were twice the magnitude of the S-T segment shifts from the other. This indicates the kind of problem that can be encountered when trying to use S-T segment deviations as a quantitative measure of the extent of myocardial injuries. Changes in the precise shapes of the boundaries of an injury can cause large changes in the surface ECG without significantly affecting the volume of the injured tissue.

Body surface mapping techniques have been proposed as more sensitive indicators of certain cardiac abnormalities than the standard 12-lead ECG.[2] Studies of isopotential maps following anterior myocardial infarction have noted the appearance of an abnormal potential minimum over the infarcted region early in ventricular activation.[12] Subjects with chronic inferior myocardial infarction have been described as having a displacement of the normal potential minimum early in activation, from the region of the right shoulder to the lower right portion of the torso.[13] Similar features can be seen in the simulated maps shown in Figure 9. S-T segment mapping procedures have been tested as a means of quantitating changes in the amount of ischemic injury following an occlusion of a coronary artery.[14] The simulated isopotential surface maps (Fig. 10) demonstrate the dependence of the potential distribution early in the S-T segment on the location of the injury. Although the S-T segment-mapping techniques tested have had only limited success,[15] information about the location of the injury is clearly contained in the simulated maps. More sophisticated processing of the surface potential data may lead to more accurate quantitative information concerning the location and extent of the myocardial injury. Since the model can be used to simulate potentials anywhere on the torso surface, it should be useful in investigating the information contained in body surface maps.

References

1. Fowler NO: Cardiac Diagnosis and Treatment. New York, Harper & Row, 1976
2. Taccardi B, DeAmbroggi L, Viganotti C: Body-surface mapping of heart potentials. *In* The Theoretical Basis of Electrocardiology, edited by CV Nelson, DB Geselowitz. London, Oxford University Press, 1976
3. Kardesch M, Hogancamp CE, Bing RJ: The effect of complete ischemia on the intracellular electrical activity of the whole mammalian heart. Circ Res **6:** 715-720, 1958
4. Samson WE, Scher AM: Mechanisms of S-T segment alteration during acute myocardial injury. Circ Res **8:** 780-787, 1960
5. Downar E, Janse MJ, Durrer D: The effect of ischemic blood on transmembrane potentials of normal porcine ventricular myocardium. Circulation **55:** 455-462, 1977
6. Mandel WJ, Burgess MJ, Neville J, Abildskov JA: Analysis of T wave abnormalities associated with myocardial infarction using a theoretic model. Circulation **38:** 178-188, 1968
7. Toyoshima HM, Printzmetal M, Horiba M, Kobayashi T, Mizuno Y, Nakayama R, Yamada K: Nature of normal and abnormal electrocardiograms: Relation of S-T segment and T wave changes to intracellular potentials. Arch Intern Med **115:** 4-16, 1965
8. Thiry PS, Rosenberg RM, Abbott JA: A mechanism for the electrocardiogram response to left ventricular hypertrophy and acute ischemia. Circ Res **36:** 92-104, 1975
9. Madias JE: The earliest electrocardiographic signs of acute transmural myocardial infarction. J Electrocardiol **10:** 193-196, 1977
10. Fenichel NM, Kugell VH: The large Q-wave of the electrocardiogram. A correlation with pathological observations. Am Heart J **7:** 235-248, 1931
11. Holland RP, Brooks H: A theoretic and experimental analysis of the TQ and S-T segment. Circ Res **37:** 471-480, 1975
12. Sugiyama S, Wada M, Sugenoya J, Toyoshima H, Toyama J, Yamada K: Experimental study of myocardial infarction through the use of body surface isopotential maps: Ligation of the anterior descending branch of the left coronary artery. Am Heart J **93:** 51-59, 1977
13. Vincent GM, Abildskov JA, Burgess MJ, Millar K, Lux RL, Wyatt R: Diagnosis of old inferior myocardial infarction by body surface isopotential mapping. Am J Cardiol **39:** 510-515, 1977
14. Braunwald E, Maroko P: S-T segment mapping: Realistic and unrealistic expectations. Circulation **54:** 529-532, 1976
15. Fozzard HA, DasGupta DS: S-T segment potentials and mapping: Theory and experiments. Circulation **54:** 534-537, 1976